

AD-A142 771

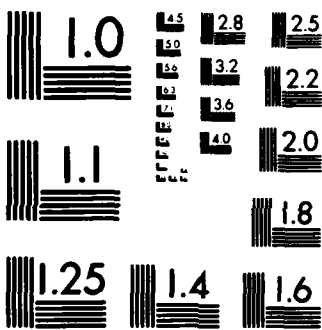
A UV-PREIONIZED KRF EXCIMER LASER WITH AN OUTPUT ENERGY 1/1
OF 042 J(U) FOREIGN TECHNOLOGY DIV WRIGHT-PATTERSON AFB
OH C YUAN ET AL. 12 AUG 82 FTD-ID(RS)T-0787-82

UNCLASSIFIED

F/G 20/5

NL





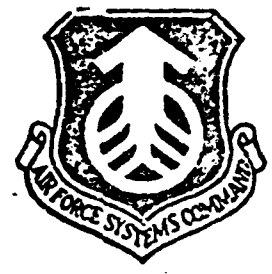
MICROCOPY RESOLUTION TEST CHART
NATIONAL BUREAU OF STANDARDS-1963-A

①

FTD-ID(RS)T-0797-52

AD-A142 771

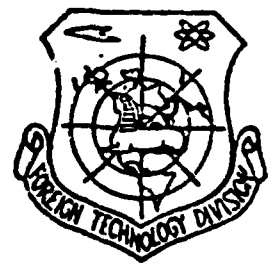
FOREIGN TECHNOLOGY DIVISION



A UV-PREIONIZED KrF EXCIMER LASER WITH AN
OUTPUT ENERGY OF 0.42 J

by

Yuan Cailai, Shangguan Chen, et al



JUL 11 1984

DTIC FILE COPY

Approved for public release;
distribution unlimited.



84 07 10 120

EDITED TRANSLATION

FTD-ID(RS)T-0787-82

12 August 1982

MICROFICHE NR: FTD-82-C-001090

A UV-PREIONIZED KrF EXCIMER LASER WITH AN OUTPUT
ENERGY OF 0.42 J

By: Yuan Cailai, Shangguan Chen, et al

English pages: 8

Source: Jiguang, Vol. 8, Nr. 12, 1981,
pp. 4-7

Country of origin: China

Translated by: SCITRAN
F33657-81-D-0263

Requester: FTD/TQTD

Approved for public release; distribution unlimited.

THIS TRANSLATION IS A RENDITION OF THE ORIGINAL FOREIGN TEXT WITHOUT ANY ANALYTICAL OR EDITORIAL COMMENT. STATEMENTS OR THEORIES ADVOCATED OR IMPLIED ARE THOSE OF THE SOURCE AND DO NOT NECESSARILY REFLECT THE POSITION OR OPINION OF THE FOREIGN TECHNOLOGY DIVISION.

PREPARED BY:

TRANSLATION DIVISION
FOREIGN TECHNOLOGY DIVISION
WP.AFB, OHIO.

GRAPHICS DISCLAIMER

All figures, graphics, tables, equations, etc, merged into this translation were extracted from the best quality copy available.



Accession For	
NTIS GRA&I	<input checked="" type="checkbox"/>
DTIC TAB	<input type="checkbox"/>
Unannounced	<input type="checkbox"/>
Justification	
Distribution	
Availability Codes	
Availability Codes	
Int	General
AI	

A UV-PREIONIZED KrF EXCIMER LASER WITH AN
OUTPUT ENERGY OF 0.42 J

Yuan Callai Shangguan Cheng Ye Chao Dou Airong Lin Yingyi
(Shanghai Institute of Optics and Fine Mechanics, Academia Sinica)

Abstract: Experimental studies on the high power and high efficiency UV-preionized KrF ($\lambda = 248\text{nm}$) excimer laser are reported. The maximum output energy per pulse is over 420 mJ. Characteristics of lasing and fluorescence spectrum for KrF are studied. The effect of additive Ne gas in the mixture on lasing energy is examined.

The KrF laser is the most representative among inert gas halide excimer lasers. It has already been reported in the literature that the output of nearly 400 millijoules was obtained by using the ultra-violet pre-ionized fast discharge excitation method.[1,2] The actual maximum output has reached 1 joule. We have constructed a UV-preionized apparatus and obtained a maximum KrF pulsed output in excess of 420 millijoules. The laser has been in operation for over a year, proving its function to be stable and reliable.

1. Experimental Set-up

The experimental set-up and principle are similar to those in reference [3]. The apparatus is constructed of glass epoxy with an internal diameter of 84mm and length 940mm. The electrodes are made of brass in the Zhang uniform field configuration. The effective region of discharge is $80 \times 2.1 \times 0.5 \text{cm}^3$. The pre-ionization spark gap plates are placed symmetrically in a upright direction at a distance of 3.8 cm from the principle discharge electrode. Each spark gap consists of 29 gaps, each of which is made of a nickel plate of length 27mm, width 5mm and thickness 0.1mm. The separation between the gaps is 1mm. The preionization capacitance is 0.047 μfd . The LC inverted circuit is used with $C_1 = 12 \text{m}\mu\text{fd}$, $C_2 = 25 \text{m}\mu\text{fd}$. The two

Received: February 26, 1981

low inductance co-axial spherical gaps are filled with N2 gas at high pressure. The delay time for trigger pulse is 1 usec.

The distance between the two reflecting mirrors is 106 cm. The resonance cavity is formed by a totally reflecting dielectric film mirror of radius of curvature 5m and a flat output plate. The output plate is made of 2 optically cemented quartz plates. A WFG-100 1 meter grating spectrograph is used to photograph the lasing spectrum and fluorescence spectrum.

2. Results and Discussions

We have studied in detail the relational curves between the laser output energy and the mixing ratio of the gaseous mixture, the total pressure, the main discharge potential, the delay time and the buffer gas. We have also studied the characteristics of the lasing and fluorescence spectra. Figure 1 shows the relationship between the laser output energy and the Kr gas content. It can be seen from the graph that for fixed F₂ content at 0.4%; the Kr content is best at 10-15%. Increasing the Kr content further will reduce the output. This may be explained from the formation of KrF excimer and quenching dynamics. There are two main ways to form KrF excimers. One is the 'Harpooning' reaction:



Kr can easily transfer the extra electrons to F₂ to form an ionic bond. The rate is of the order 10⁻⁹cm³/sec. The other way is 3 body collision recombination





where M is the buffer gas. It maybe He, Ne, Ar, etc. The reaction rate is also about $10^{-9} \text{cm}^3 \text{sec}^{-1}$ (4). From (3) it can be seen that when the Kr content increases, the growth of KrF will also increase. The principle quenching mechanism of KrF is

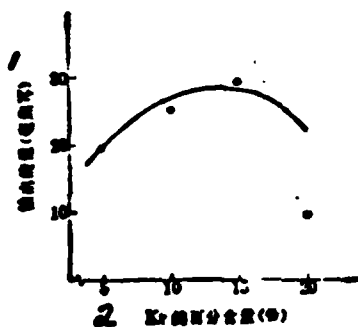


Figure 1. Relation between output power and various Kr contents.

Key: 1--output energy (millijoule); 2--percent content of Kr (%).

F_2 : 0.4%, total pressure: 1 atmosphere

Main discharge potential: 17 Kv

He is the gas

Preionization potential: 18 Kv.

From (5), it may be seen that too much Kr gas content, the 3 body collision quenching rate will increase. By combining (3) and (5), it may be seen that a best Kr content exists. Similarly from (1), (2) and (4), it may also be seen that a best F_2 content also exists. When the total pressure is at 3 atmosphere, the main discharge potential at 50 kilovolts, Kr content at 13%, He content at 51%, Ne content at 35.65%, the best F_2 content is at 0.35%. Figure 2 and Figure 3 show the relationship between laser output energy and total gas pressure. Under the experimental conditions as indicated in the diagrams, it can be seen in Figure 2 that when the main discharge potential is 42.5-47 Kv, the laser output energy increases with the total gas pressure. When the main discharge potential is 32Kv, the output increases linearly with the total gas pressure. However, from 1.6 atmospheres on, saturation is gradually approached and the peak value reached, and the output then decreases with the rising pressure. From Figure 3, we can find $(E/P)_{\text{optimal}} = 10 \text{ volt/cm. torr.}$ Hence, in our apparatus, it may still be possible to increase the laser output energy by further increasing the total gas pressure under the current main discharge potential value of 50 Kv. Figure 4 shows the relationship between output laser energy and main discharge potential at various total gas pressures. When the fixed preionizing potential is 20 Kv and $F_2:Kr:He = 0.2\%:13\%:87\%$ it may be seen in the diagram that the laser energy increases almost linearly with the main discharge potential. After the potential reaches 45 Kv, the rise gradually diminishes and this increase begins to flatten with the decrease of the total gas pressure.

/6

Figure 5 shows the relationship of the output lasing energy and the time delay between the main discharge potential and preionizing potential. From the diagram, one can see that the delay time between the main discharge and preionization is 1 microsecond, the laser output obtained is the largest. With the increase of the delay time, the output decreases nearly linearly.

The effect of the buffer gas in the excimer laser is important. In reference [5], the replacement of He by Ne doubles the laser energy. In reference [6], the introduction in the gas mixture of 10% Ar and 1%

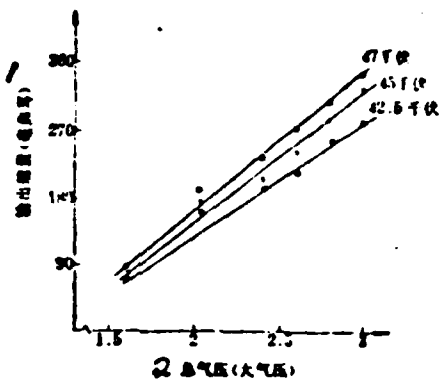


Figure 2. Relationship between output energy and total gas pressure.

Key: 1--output energy (millijoule); 2--total gas pressure (atmosphere).

$F_2=0.2\%$; Kr:13%; He is the gas; preionizing potential: 20 Kv.

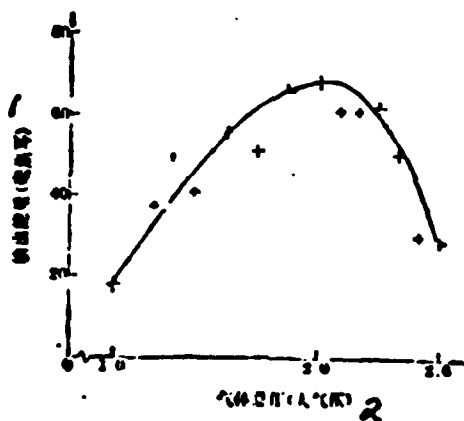


Figure 3. Variational relationship between output laser energy and total gas pressure.

Key: 1--output energy (millijoule); 2--total gas pressure (atmosphere).

Main discharge potential: 32 Kv.

Preionizing potential: 20 Kv.

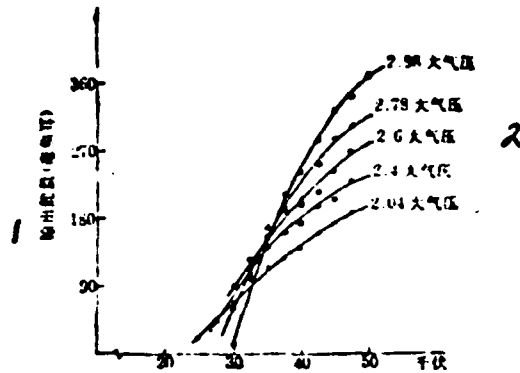


Figure 4. Relationship between output energy and main discharge potential at various total gas pressure $F_2:0.2\%$; $Kr:13\%$; He is the buffer gas.

Key: 1--output energy (millijoule); 2--2.98 atmosphere
 2.78 atmosphere
 2.6 atmosphere
 2.4 atmosphere
 2.04 atmosphere

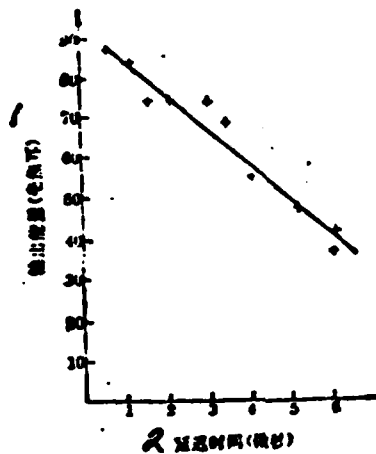


Figure 5. Relation curve between output energy and delay time.
 Key: 1--output energy (millijoule); 2--delay time (microsec).
 Main discharge potential: 30 .Kv.
 Total gas pressure 2.5 atmosphere.

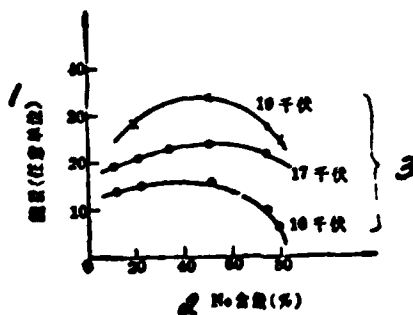


Figure 6. Relation between output energy and Ne content.
 Key: 1--energy (arbitrary unit); 2--Ne content (%); 3-- 19Kv
 17Kv
 16Kv
 Total pressure: 3 atmospheres.

Ne raises the output energy by 20%. We investigated the effect of adding He and Ne of various proportions in the gaseous mixture on the laser output. The results are shown in Figure 6. From Figure 6, it can be seen that by adding 50% Ne to the gaseous mixture, the laser output energy may be increased by about 40%. We used a gas mixture of 0.35%F, 13.3%Kr 35%Ne and 51.35%He, a total gas pressure of 3 atmosphere, main discharge potential 51.5 Kv, pre-ionizing potential 21 Kv and obtained a maximum pulsed output energy of 424 millijoule. The efficiency $(E_{out} / \frac{1}{2}(O_1 + O_2)V^2)$ is about 1%. Energy density is 5 joules/litre. In the experiment, the total reflecting dielectric film and aluminum film reflectors are found to have apparent laser damage. The damage on the dielectric film is less than that on the aluminum film. This may possibly be due to the absorption of UV wave length by the film.

We photographed the KrF* fluorescence spectrum and lasing spectrum with a WPG-100 one meter grating spectrograph, as shown in Figure 7. From the diagram, we may see that the width of the fluorescence spectrum is 32 Å, and the lasing line width 7 Å.

In the neighborhood of 249 millimicron, there is an absorption peak in both the fluorescence and the lasing spectrum. The central wavelength of the laser line is 248 millimicron. This is KrF* (B→X) transition. We have also observed a fluorescence spectrum near 222 millimicron. This is KrF* (D→X) transition. The central wavelength of the transition is 221.5 millimicron, and the fluorescence width is 20 Å, somewhat different from the KrF* (D→X) transition wavelength of 220 millimicron as reported in reference [7].

17

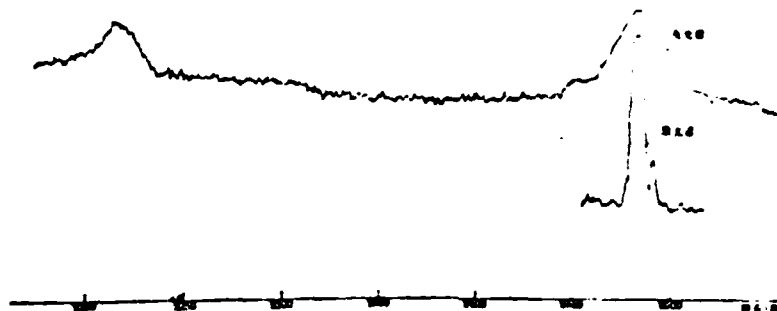


Figure 7. Fluorescence and lasing spectra of KrF.

Fluorescence spectrum — total pressure: 1.5 atmosphere; main discharge; potential: 16Kv, Slit: 0.3mm; 100 exposures.

Lasing spectrum — total pressure: 2 atmospheres; main discharge potential: 35Kv; Slit: 5 micron; 1 exposure.

References

- [1]. R.C. Sze et al.; IEEE J. Quant. Electr., 1979, QE-15, 1338.
- [2]. D.E. Rothe et al.; IEEE J. Quant. Electr., 1979, QE-15, 314.
- [3]. Shangguan Cheng, et al.: (Laser) 1981, 8, No. 2, 17.
- [4]. C.K. Rhodes; Topics Appl. Phys. 1979, 30, 97-98, Springer-Verlag Berlin Heidelberg N.Y.
- [5]. T.S. Fablen; IEEE J. Quant. Electr., 1979, QE-15, 311.
- [6]. R.C. Sze et al.; IEEE J. Quant. Electr., 1978, QE-14, 944.
- [7]. J.R. Murray, et al.; Appl. Phys. Lett., 1976, 29, 252. J.E. Velazco et al.; J. Chem. Phys., 1976, 65, 3468.

DISTRIBUTION LIST

DISTRIBUTION DIRECTOR'S OFFICE

ORGANIZATION

MICROFILM

A205 LMAVIC	1
A210 LMAVIC	1
B344 DIA/RTS-2C	9
C043 USAMIIA	1
C500 TRADOC	1
C509 BALLISTIC RES LAB	1
C510 R&T LABS/AVRADCOM	1
C513 AVRADCOM	1
C535 AVRADCOM/TSARCOM	1
C539 TRASANA	1
C591 ESTC	4
C619 MIA REDSTONE	1
D008 NISC	1
E053 HQ USAF/INLET	1
E403 AFSC/INA	1
E404 AEDC/DOF	1
E408 AFWL	1
E410 AD/IND	1
E429 SD/IND	1
P005 DOE/ISA/DDI	1
P050 CIA/OCR/ND/SD	2
AFIT/LDE	1
FTD	
CCN	1
NIA/PHS	1
NIIS	2
LIJNL/Code L-389	1
NASA/NST-44	1
NSA/1213/TDL	2

REPROD

FILMED

8

11